Advances in Solid Oxide Fuel Cells V

A Collection of Papers Presented at the 33rd International Conference on Advanced Ceramics and Composites January 18–23, 2009 Daytona Beach, Florida

Edited by
Narottam P. Bansal
Prabhakar Singh

Volume Editors
Dileep Singh
Jonathan Salem

A John Wiley & Sons, Inc., Publication

This Page Intentionally Left Blank

Advances in Solid Oxide Fuel Cells V

This Page Intentionally Left Blank

Advances in Solid Oxide Fuel Cells V

A Collection of Papers Presented at the 33rd International Conference on Advanced Ceramics and Composites January 18–23, 2009 Daytona Beach, Florida

Edited by
Narottam P. Bansal
Prabhakar Singh

Volume Editors
Dileep Singh
Jonathan Salem

A John Wiley & Sons, Inc., Publication

Published by John Wiley & Sons, Inc., Hoboken, New Jersey.
Published simultaneously in Canada.

Library of Congress Cataloging-in-Publication Data is available.

ISBN 978-0-470-45754-2

Printed in the United States of America.

10 9 8 7 6 5 4 3 2 1

Contents

ELECTRODES

OXIDE/PROTON CONDUCTORS

SEALS

MECHANICAL BEHAVIOR

MATERIALS SYNTHESIS

FUEL REFORMING

This Page Intentionally Left Blank

Preface

The Sixth International Symposium on Solid Oxide Fuel Cells (SOFC): Materials, Science, and Technology was held during the 33rd International Conference and Exposition on Advanced Ceramics and Composites in Daytona Beach, FL, January 18 to 23, 2009. This symposium provided an international forum for scientists, engineers, and technologists to discuss and exchange state-of-the-art ideas, information, and technology on various aspects of solid oxide fuel cells. A total of 112 papers were presented in the form of oral and poster presentations, including ten invited lectures, indicating strong interest in the scientifically and technologically important field of solid oxide fuel cells. Authors from 17 countries (Brazil, Canada, China, Denmark, France, Georgia, Germany, India, Italy, Japan, Romania, Russia, Singapore, South Korea, Taiwan, United Kingdom, and U.S.A.) participated. The speakers represented universities, industries, and government research laboratories.

These proceedings contain contributions on various aspects of solid oxide fuel cells that were discussed at the symposium. Twenty four papers describing the current status of solid oxide fuel cells technology and the latest developments in the areas of fabrication, characterization, testing, performance, electrodes, electrolytes, seals, cell and stack development, proton conductors, fuel reforming, mechanical behavior, powder synthesis, etc. are included in this volume. Each manuscript was peer-reviewed using The American Ceramic Society review process.

The editors wish to extend their gratitude and appreciation to all the authors for their contributions and cooperation, to all the participants and session chairs for their time and efforts, and to all the reviewers for their useful comments and suggestions. Financial support from The American Ceramic Society is gratefully acknowledged. Thanks are due to the staff of the meetings and publications departments of The American Ceramic Society for their invaluable assistance. Advice, help and cooperation of the members of the symposium's international organizing committee (Tatsumi Ishihara, Tatsuya Kawada, Nguyen Minh, Mogens Mogensen, Nigel Sammes, Robert Steinberger-Wilkens, Jeffry Stevenson, and Eric Wachsman) at various stages were instrumental in making this symposium a great success.

It is our earnest hope that this volume will serve as a valuable reference for the engineers, scientists, researchers and others interested in the materials, science and technology of solid oxide fuel cells.

NAROTTAM P. BANSAL
NASA Glenn Research Center

PRABHAKAR SINGH
University of Connecticut

Introduction

The theme of international participation continued at the 33rd International Conference on Advanced Ceramics and Composites (ICACC), with over 1000 attendees from 39 countries. China has become a more significant participant in the program with 15 contributed papers and the presentation of the 2009 Engineering Ceramic Division's Bridge Building Award lecture. The 2009 meeting was organized in conjunction with the Electronics Division and the Nuclear and Environmental Technology Division.

Energy related themes were a mainstay, with symposia on nuclear energy, solid oxide fuel cells, materials for thermal-to-electric energy conversion, and thermal barrier coatings participating along with the traditional themes of armor, mechanical properties, and porous ceramics. Newer themes included nano-structured materials, advanced manufacturing, and bioceramics. Once again the conference included topics ranging from ceramic nanomaterials to structural reliability of ceramic components, demonstrating the linkage between materials science developments at the atomic level and macro-level structural applications. Symposium on Nanostructured Materials and Nanocomposites was held in honor of Prof. Koichi Niihara and recognized the significant contributions made by him. The conference was organized into the following symposia and focused sessions:

Symposium 1	Mechanical Behavior and Performance of Ceramics and Composites
Symposium 2	Advanced Ceramic Coatings for Structural, Environmental, and Functional Applications
Symposium 3	6th International Symposium on Solid Oxide Fuel Cells (SOFC): Materials, Science, and Technology
Symposium 4	Armor Ceramics
Symposium 5	Next Generation Bioceramics
Symposium 6	Key Materials and Technologies for Efficient Direct Thermal-to-Electrical Conversion
Symposium 7	3rd International Symposium on Nanostructured Materials and Nanocomposites: In Honor of Professor Koichi Niihara
Symposium 8	3rd International symposium on Advanced Processing & Manufacturing Technologies (APMT) for Structural & Multifunctional Materials and Systems

Symposium 9	Porous Ceramics: Novel Developments and Applications
Symposium 10	International Symposium on Silicon Carbide and Carbon-Based Materials for Fusion and Advanced Nuclear Energy Applications
Symposium 11	Symposium on Advanced Dielectrics, Piezoelectric, Ferroelectric, and Multiferroic Materials
Focused Session 1	Geopolymers and other Inorganic Polymers
Focused Session 2	Materials for Solid State Lighting
Focused Session 3	Advanced Sensor Technology for High-Temperature Applications
Focused Session 4	Processing and Properties of Nuclear Fuels and Wastes

The conference proceedings compiles peer reviewed papers from the above symposia and focused sessions into 9 issues of the 2009 Ceramic Engineering & Science Proceedings (CESP); Volume 30, Issues 2-10, 2009 as outlined below:

- Mechanical Properties and Performance of Engineering Ceramics and Composites IV, CESP Volume 30, Issue 2 (includes papers from Symp. 1 and FS 1)
- Advanced Ceramic Coatings and Interfaces IV Volume 30, Issue 3 (includes papers from Symp. 2)
- Advances in Solid Oxide Fuel Cells V, CESP Volume 30, Issue 4 (includes papers from Symp. 3)
- Advances in Ceramic Armor V, CESP Volume 30, Issue 5 (includes papers from Symp. 4)
- Advances in Bioceramics and Porous Ceramics II, CESP Volume 30, Issue 6 (includes papers from Symp. 5 and Symp. 9)
- Nanostructured Materials and Nanotechnology III, CESP Volume 30, Issue 7 (includes papers from Symp. 7)
- Advanced Processing and Manufacturing Technologies for Structural and Multifunctional Materials III, CESP Volume 30, Issue 8 (includes papers from Symp. 8)
- Advances in Electronic Ceramics II, CESP Volume 30, Issue 9 (includes papers from Symp. 11, Symp. 6, FS 2 and FS 3)
- Ceramics in Nuclear Applications, CESP Volume 30, Issue 10 (includes papers from Symp. 10 and FS 4)

The organization of the Daytona Beach meeting and the publication of these proceedings were possible thanks to the professional staff of The American Ceramic Society (ACerS) and the tireless dedication of the many members of the ACerS Engineering Ceramics, Nuclear & Environmental Technology and Electronics Divisions. We would especially like to express our sincere thanks to the symposia organizers, session chairs, presenters and conference attendees, for their efforts and enthusiastic participation in the vibrant and cutting-edge conference.

DILEEP SINGH and JONATHAN SALEM
Volume Editors

Cell and Stack Development/Performance

This Page Intentionally Left Blank

DEVELOPMENT OF NOVEL PLANAR NANO-STRUCTURED SOFCs

Tim Van Gestel, Doris Sebold, Wilhelm A. Meulenberg, Hans-Peter Buchkremer
Forschungszentrum Jülich GmbH, Institute of Energy Research, IEF-1: Materials Synthesis and Processing, Leo-Brandt-Strasse, D-52425 Jülich, Germany

ABSTRACT

This paper reports a study on the preparation of thin nano-structured 8YSZ membrane films by nano-dispersion and sol-gel coating methods. For the deposition process, four different coating liquids with varying particle size, covering the range from 85 nm to 6 nm, were prepared. In the first part, it is demonstrated that nano-dispersions with a particle size of e.g. 85 or 65 nm can be used for the formation of dense YSZ membranes with a thickness of 1 – 2 μm, but the layers can only be sintered to full density at 1400°C. In the second part, ultra-thin YSZ membranes are prepared by sol-gel coating (particle size 35 and 6 nm). These layers show a thickness < 500 nm and a very tight mesoporous or microporous structure in the calcined state (pore size < 5 nm), which leads to sintered membrane layers in the desired temperature range (~ 1200°C). In the final part, it is described by means of He leak tests that on the applied large-scale state-of-the-art substrate with a high surface roughness, a firing temperature of 1300°C is however required to sinter the membranes to full density.

INTRODUCTION

At Forschungszentrum Jülich (FZJ), an advanced planar anode supported SOFC has been developed, characterized by an average power output of 1.4 W/cm^2 at 750°C and 0.7 V. The typical multilayer structure of the FZJ cell comprises: (1) a porous 8YSZ/NiO anode substrate with an area of 20 x 20 cm^2; (2) a porous 8YSZ/NiO anode functional layer; (3) a dense 8YSZ electrolyte layer with a thickness in the range 5 – 10 μm; (4) a porous LSM or LSCF cathode. In the standard manufacturing procedures, the substrate is made by warm pressing or tape-casting and, subsequently, the respective layers are deposited from a suspension by means of vacuum slip-casting, screen-printing or wet-powder spraying.

Currently, one of the main objectives in our research is to produce novel electrolyte membrane layers, which can be sintered to full density at a lower temperature than currently applied in SOFC manufacturing (> 1400°C). This will reduce significantly the production cost of the cell and permit the use of steel substrates to build up the cell.

In this paper, nano-dispersion and sol-gel coating procedures are described and their potential for SOFC manufacturing is discussed. In our related research group 'separation membranes', such coating procedures are already used for several years as a method of producing thin mesoporous (pore size > 2 nm) and microporous (pore size < 2 nm) membrane films of several materials including electrolyte materials (e.g. $3Y_2O_3$-ZrO_2, $8Y_2O_3$-ZrO_2, $10Gd_2O_3$-CeO_2) [1]. The pore size of such membrane films can be varied in the range from ~ 20 nm down to even smaller than 1 nm - depending on the particle size of the coating liquid - and is considerably smaller than the pore size of a macroporous membrane films made by a conventionally used suspension deposition procedure.

From a practical point of view, coating of sols and nano-dispersions appears also as an interesting method for SOFC manufacturing, since the coating methods are the same as conventional suspension methods and exhibit the same advantages (inexpensive in terms of capital costs, simplicity of the equipment). The basic question when considering these new thin-film coating methods includes, however, how to deal with a regular anode substrate showing an inferior surface quality when compared with substrates usually used for thin film deposition. As shown in Figure 1, the thickness of the 8YSZ electrolyte layer, which is

normally deposited on our anode layer by a powder procedure, measures ~ 10 μm after sintering.

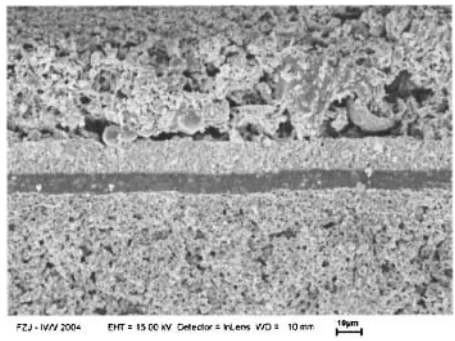

Fig. 1. SEM micrograph of the standard SOFC prepared at FZJ with 8YSZ/NiO anode substrate, 8YSZ/NiO anode layer, 8YSZ electrolyte, 8YSZ/LSM cathode layer and LSM cathode (bar = 10 μm).

EXPERIMENTAL

1. Anode Substrate

The standard anode produced at our institute (IEF-1), which consists of a warm-pressed 8YSZ/NiO plate and a relatively thin vacuum slip-casted macroporous 8YSZ/NiO layer, is used as substrate in all coating experiments. From Figure 1, it appears that the thickness of the anode layer measures ~ 10 μm; the thickness of the supporting plates was 1 mm or 1.5 mm in all experiments.

In Figure 2a, the pore size distribution of the substrate is shown. From this graph, an average pore size of ~ 0.7 – 0.8 μm (large peak) and ~ 200 – 300 nm (small peaks) is evident for the substrate plate and for the anode layer, respectively.

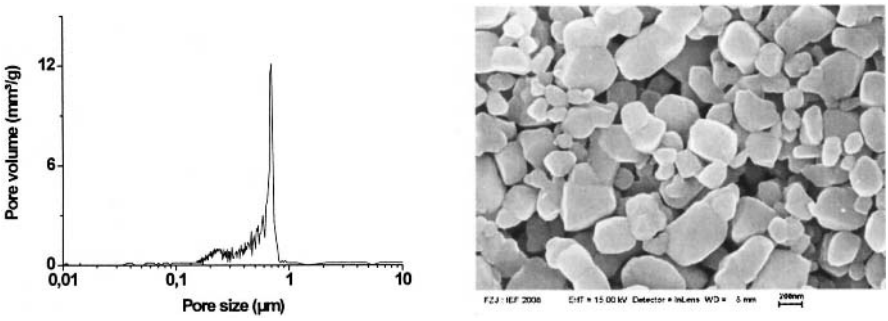

(a) (b)

Fig. 2a. Pore size distribution of test substrate consisting of a 8YSZ/NiO anode plate and a 8YSZ/NiO anode layer. Figure 2b. Surface micrograph of the anode layer.

Figure 2b shows a detail surface micrograph of the anode layer. This micrograph confirms a typical macroporous structure with a particle size in the range 200 – 400 nm and an average pore size in the range 200 – 300 nm. Further, it is also confirmed that the anode layer shows a wide pore size distribution.

2. Preparation of the coating liquids

As shown in previous coating experiments, deposition of continuous membrane layers on this kind of anode requires a coating liquid containing relatively large particles [2]. In a series of coating experiments, dense 8YSZ electrolyte layers with a thickness in the range 1 - 4 μm could be deposited, when the coating liquid was a dispersion with a particle size of ~ 200 nm and PVA was added as coating additive (coating methods included dip-coating, vacuum-casting and spraying). The main drawback of our proposed coating procedure was however the requirement of a high sintering temperature of 1400°C for these 8YSZ membranes, similar to the sintering temperature of conventional electrolyte layers. In this paper, a new series of coating experiments with four different coating liquids - including two nano-dispersions and two sols - is described, in order to check the effect of a decreasing particle size on the sintering behaviour of the electrolyte membrane layer.

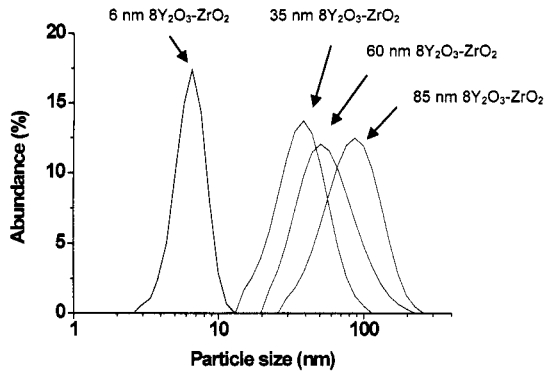

Fig. 3. Particle size distribution of nano-dispersions and sols descirbed in this work

A first nano-dispersion was made starting from a commercially available 8YSZ nano-powder (Evonik Degussa) and an aqueous nitric acid solution. Characterization of the particle size was done by dynamic laser beam scattering (Horiba LB-550) in a similar way as in our previous work (1) and here an average particle size of ~ 85 nm was measured. A coating liquid was prepared from this dispersion by adding polyvinyl alcohol (PVA) as coating and drying controlling additive. Subsequently, a second nano-dispersion with a particle size of ~ 65 nm was prepared, using a 8YSZ nano-powder supplied by Sigma-Aldrich.

The third coating liquid was a 'so-called' colloidal sol. The sol was prepared starting from a metal organic precursor ($Zr(n\text{-}OC_3H_7)_4$, Aldrich), by means of hydrolysis and condensation of this precursor in isopropanol-water-HNO_3 solutions at 98°C. Yttria-doping (8 mol% yttria) was done by adding the proper amount of $Y(NO_3)_3.6H_2O$ to the zirconia sol. In this procedure, the size of the particles in the sol was controlled by the time of the aging process and the best results were obtained for particles with an average size of ~ 30 – 40 nm.

The fourth coating liquid in this study was a 'so-called' polymeric sol, which contains particles with a size in the nanometer range. This sol was produced by controlled hydrolysis

of $Zr(n\text{-}OC_3H_7)_4$, in the presence of diethanol amine (DEA) as a precursor modifier/polymerization inhibitor and an yttrium precursor ($Y(i\text{-}OC_3H_7)_3$) as a doping compound. The essential feature of the preparation route is the addition of DEA, which leads to a reproducible formation of nano-particles with a size of 5 - 10 nm in the synthesis process and also acts as a coating and drying controlling additive [3]. In Figure 3, an overview of the size distributions measured by dynamic laser scattering of the prepared sols and nano-dispersions is shown.

3. Membrane coating

Dip-coating experiments were performed using an automatic dip-coating device, equipped with a holder for 4 x 4 cm^2 substrates. The anode substrates were cut from calcined anode plates obtained from our standard production process (calcination temperature 1000°C, dimension 25 x 25 cm^2). In the dip-coating process, sol particles were deposited as a membrane film by contacting the upper-side (anode layer side) of the substrate with the coating liquid, while a small under-pressure was applied at the back-side. The obtained supported gel-layers were fired in air at 500°C for 2 h and then the coating – calcination cycle was repeated once, unless stated otherwise. A final sintering treatment was carried out at a temperature of 1400°C, 1300°C or 1200°C.

For He leak test measurements, 75 x 75 mm^2 anode substrates were cut and these were coated by means of a spin-coating device. In this procedure, a few ml of the coating liquid was dropped onto the substrate, which was held to the spin-coating device by means of a vacuum holder. After 30s, the substrate was then spun at high speed (1200 rpm, spinning time 1 minute). The obtained supported gel-layers were then fired in the same way as described above. Further, it should be mentioned that all coating procedures – dip-coating and spin-coating – were carried out in a clean-room.

RESULTS AND DISCUSSION

1. 85 nm 8YSZ Nano-dispersion

Figures 4a and 4b show an overview and a detail micrograph of a membrane layer obtained by coating the first nano-dispersion with a particle size of ~ 85 nm (calcination temperature 500°C). From these micrographs, a typical graded membrane structure can be observed comprising subsequently the calcined 8YSZ layer, the macroporous anode layer and the supporting anode plate. The coated 8YSZ layer is in this back-scattering type of SEM micrograph visible as a brighter film, due to its much smaller pore size. Further, it appears that a separate and continuous layer was obtained, which uniformly covers the anode layer.

By looking at the detail micrograph 4b, it appears clearly that infiltration of 8YSZ particles into the macropores of the anode layer could be prevented, by applying a plastic compound (PVA) as an additive in the coating liquid. In this micrograph, a separation line between the successive membrane layers is also visible and it appears that the thickness of a single layer obtained by one coating – calcination step measures ~ 2 – 3 μm.

The evolution of the structure of the calcined 8YSZ membrane layer at higher temperatures is shown in Figures 4c – 4f. According to the first cross-section micrograph in 4c, a dense membrane layer was obtained at a reduced firing temperature of 1300°C. However, after examanition of the surface micrographs, it appeared that densification had only proceeded to some extent (Figure 4d).

In the micrographs taken after firing at 1400 °C, a fully sintered layer was observed and much larger sintering grains are visible (Figure 4f). From all these micrographs, it was thus concluded that the coating procedure was effective - very thin dense electrolyte films

with a thickness of ~ 2 μm were obtained - but our attempt to make a dense electrolyte membrane layer at a temperature < 1400°C was not succesfull.

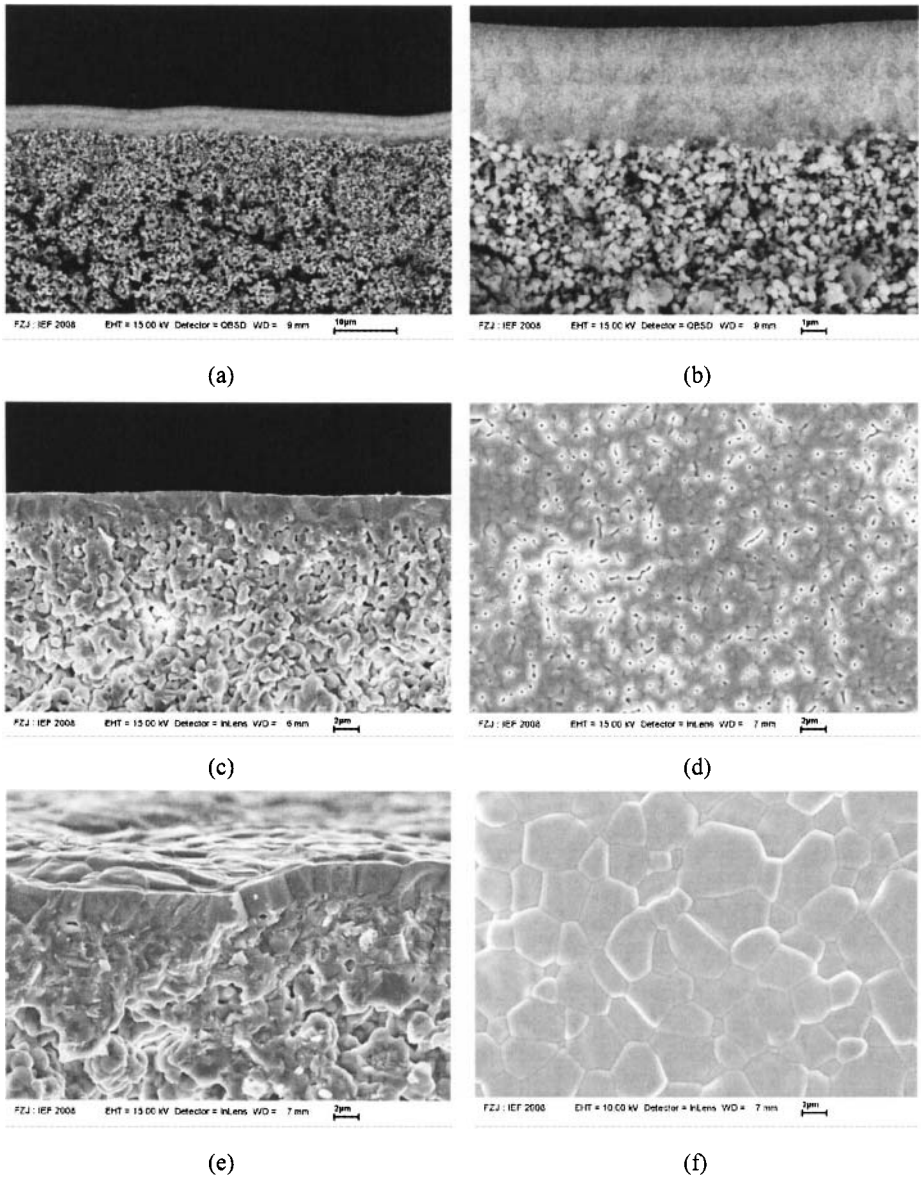

Fig. 4a and 4b. Micrographs of a calcined mesoporous $8Y_2O_3$-ZrO_2 membrane layer, obtained by dip-coating nano-dispersion 1 on the standard anode substrate. Figure 4c and 4d. Micrographs of the membrane after firing at 1300°C. Fig. 4e and 4f.. Micrographs of the membrane after firing at 1400°C.
(Layers made by 2 x dip-coating and calcination at 500°C; (a) bar = 10 μm, (b) bar = 1 μm, (c,d,e,f,) bar = 2 μm)

2. 65 nm 8YSZ Nano-dispersion

Figure 5 shows micrographs of a calcined 8YSZ membrane layer which was prepared with a nano-dispersion containing smaller particles (size ~ 65 nm). In analogy with the previous coating experiment, a continuous membrane layer was formed and infiltration of the smaller particles into the pores of the macroporous anode layer did also not occur.

The main differences with the previous coating experiment included a decreased overall membrane thickness in the calcined state of ~ 2 μm and - as shown in surface micrographs 5c and 5d - a calcined layer with a significantly finer mesoporous structure was obtained.

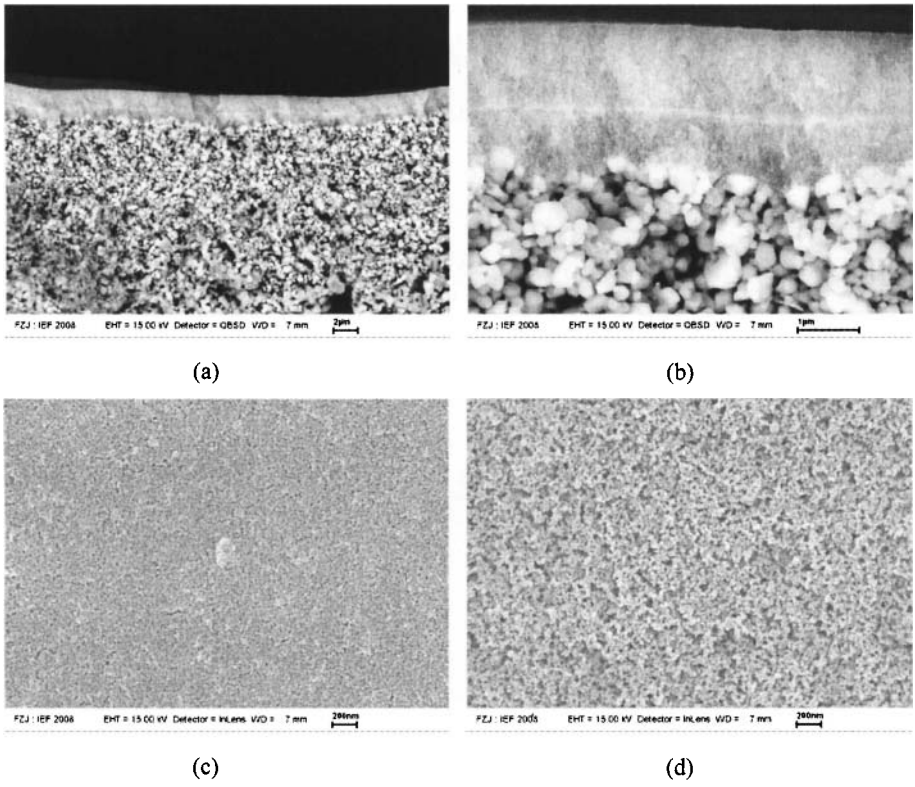

Fig. 5a and 5b. Micrographs of the cross-section of a 8YSZ membrane, obtained by dip-coating nano-dispersion 2 on the standard anode substrate. Fig. 5c and 5d. Comparison of the surface of 8YSZ membranes, obtained by dip-coating nano-dispersion 2 (5c) and nano-dispersion 1 (5d).
(Layers made by 2 x dip-coating and calcination at 500°C; (a) bar = 2 μm, (b) bar = 1, (c,d) bar = 200 nm)

As shown in Figures 6a, 6b and 6c, complete sintering required however also in this case a firing temperature of 1400°C. From the first sintering experiment at 1200°C, it appeared that densification had already proceeded to a larger extent when compared with the previous coating experiment, but the layer still contained a significant amount of pores. Further, as shown in Figure 6a (d), the membrane layer still contained a number of locally untight areas, especially at places where the surface of the substrate shows strong curvatures.

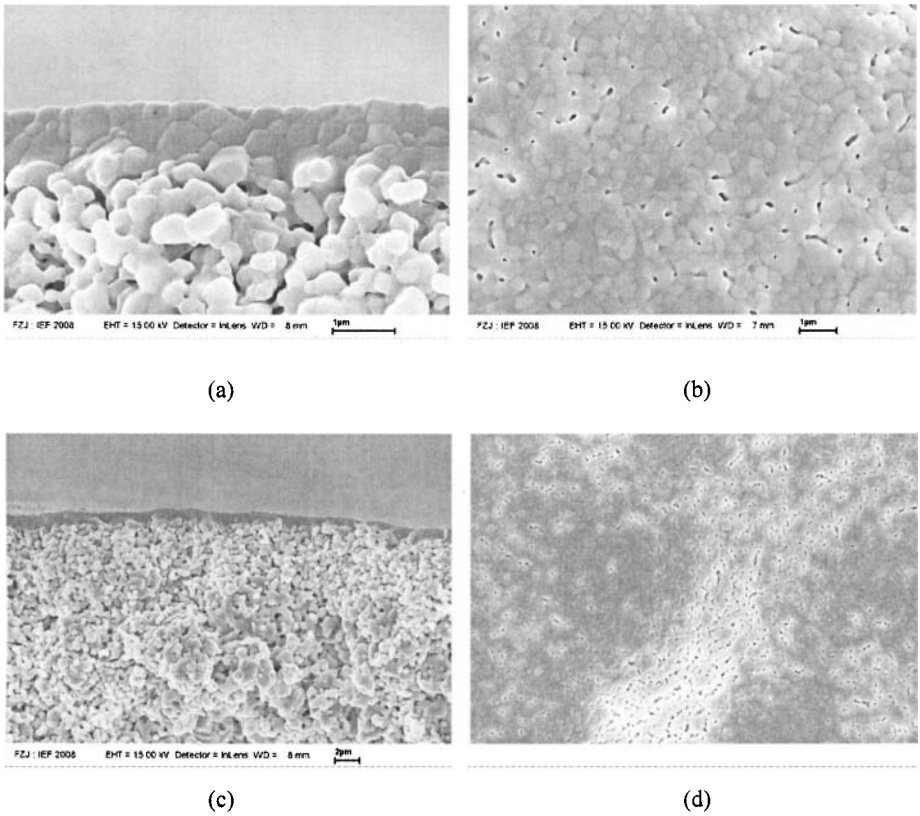

Fig. 6a (a) – (d). Micrographs of the cross-section and surface of the membrane shown in Figure 5 after firing at 1200°C.
(Layers made by 2 x dip-coating, calcination at 500°C; (a,b) bar = 1 μm, (c,d) bar = 2 μm)

After firing at 1300°C, larger grains were formed and a sintered layer with a thickness of ~ 1 μm was observed, which looked fully sintered in the detail SEM surface micrographs (Figures 6b (a)-(d)). However, after checking overview surface micrographs taken at a lower magnification (6b (e)), we still could observe a number of untight areas. In Figure 6b (f), an example of such an area is shown.

In the micrographs taken after firing at 1400°C, larger sintering grains became visible and the layer appeared completely dense, also in overview SEM pictures. From the cross-section picture in 6c (a), a final thickness of ~ 1 μm can be estimated, while the second picture of the layer at a smaller magnification in 6c (c) shows a somewhat larger thickness of ~ 1.5 μm. Anyway, it was again concluded that the coating procedure was effective - very thin dense electrolyte films with a thickness of 1 – 1.5 μm were obtained - but also this attempt to make a dense electrolyte membrane layer at a temperature < 1400°C was not succesfull. It should also be noticed that also the anode layer appears as a dense sintered layer in these SEM pictures, but He leak tests showed afterwards that the anode is only partially sintered. Further, before the finished cells are send for cell measurements, we also subject them to an additional firing in reduced atmosphere.

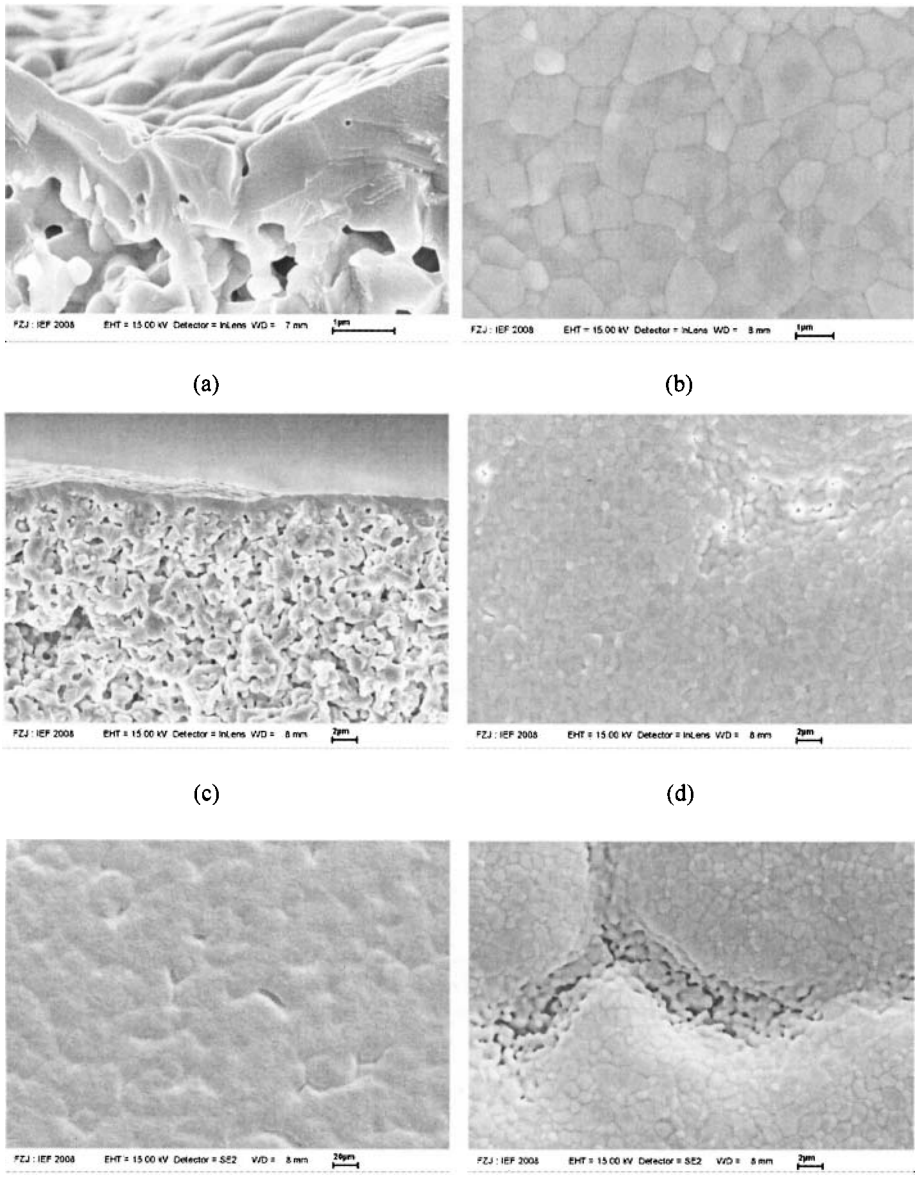

Fig. 6b (a) – (f). Micrographs of the cross-section and surface of the membrane shown in Figure 5 after firing at 1300°C
(Layers made by 2 x dip-coating, calcination at 500°C; (a,b) bar = 1 μm, (c,d,f) bar = 2 μm, (e) bar = 20 μm)

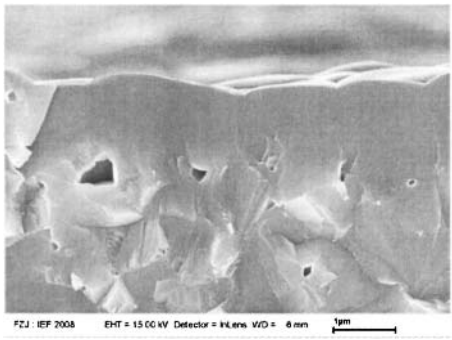

(a)

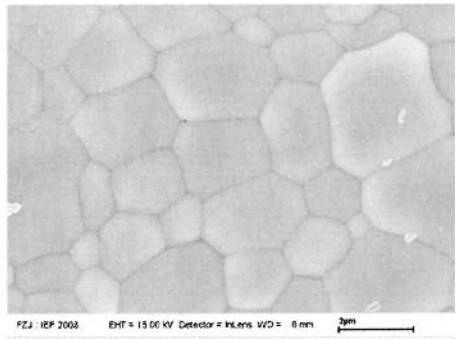

(b)

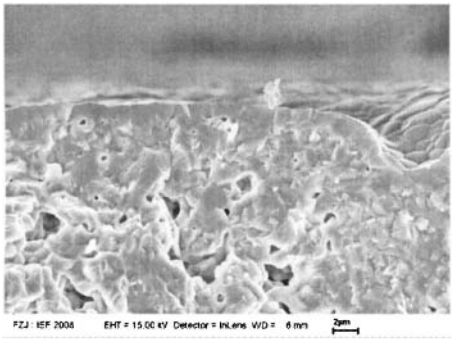

(c)

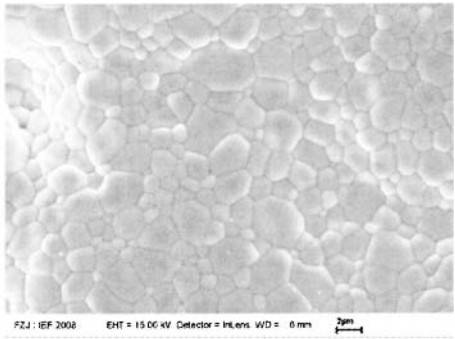

(d)

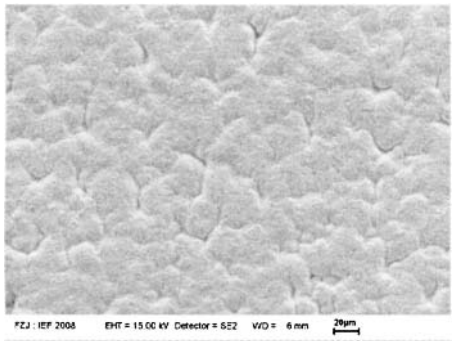

(e)

Fig. 6c (a) – (e). Micrographs of the cross-section and surface of the membrane shown in Figure 5 after firing at 1400°C.
(Layers made by 2 x dip-coating, calcination at 500°C; (a,b) bar = 1 µm, (c,d) bar = 2 µm, (e) bar = 20 µm)

3. 8YSZ Nano-dispersion + 35 nm Colloidal sol

After analysis of the previous results - a large particle size is required for the formation of a membrane layer on a very porous substrate, while sintering is improved by decreasing the particle size of the coating liquid - graded membranes, consisting of different layers with a systematically decreasing particle and pore size were developed.

In order to reduce the pore size and roughness of the substrate, a first YSZ membrane layer was deposited using nano-dispersion 2 with an average particle size of ~ 65 nm. This first layer shows a much smoother surface as the anode layer and a strongly decreased pore size of ~ 7 nm (Figure 7). Then, a second layer was deposited according to a so-called colloidal sol-gel coating procedure. As shown in the micrograph given in Figure 8a, a rather thin membrane layer with an average thickness of ~ 0.3 – 0.4 μm was obtained and the finer sol particles (average size ~ 35 nm) gave clearly a membrane layer with a smaller pore size. The separation between the two successively coated sol-gel layers can also be easily detected and it can be estimated that a single sol-gel layer is ~ 200 nm in thickness.

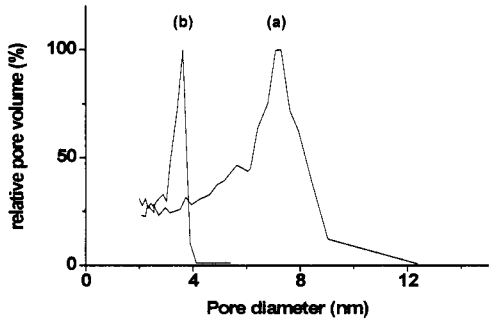

Fig. 7. Pore size distribution of the mesoporous membrane materials after calcination at 500°C.
((a) Nano-dispersion material; (b) Colloidal sol-gel material)

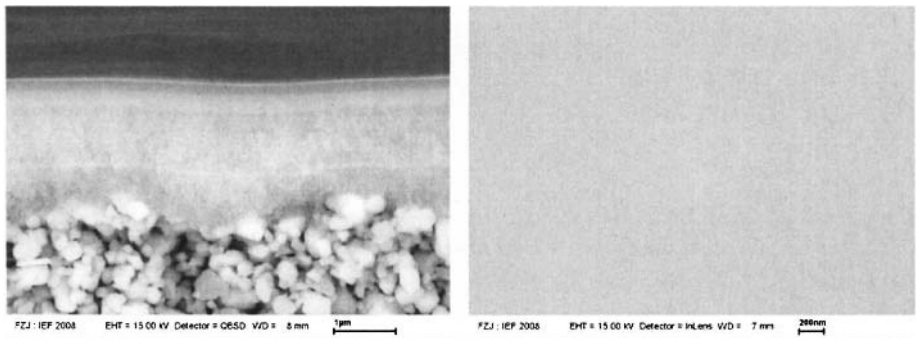

(a) (b)

Fig. 8a and 8b. Cross-section and surface of a mesoporous 8YSZ membrane, obtained by dip-coating subsequently nano-dispersion 2 and a colloidal sol.
(Layers made by 2 x dip-coating and calcination at 500°C; (a) bar = 1 μm, (b) bar = 200 nm)

Pore analysis of the sol-gel membrane material with N_2-adsorption/desorption measurements indicated a mesoporous structure (type IV isotherm) with a pore size maximum of ~ 3 - 4 nm (Figure 7), while the pore size of the first layer measures ~ 7 nm. By comparing the surface of the first layer in Figure 5c and this of the second sol-gel derived layer in Figure 8b, a clear reduction in pore size and particle size after deposition of the sol-gel layer was also confirmed.

Figure 9 shows cross-section and surface micrographs of the graded membrane after further firing at 1200°C, 1300°C and 1400°C. From the first sintering experiment at 1200°C, it appeared clearly that densification had proceeded to a much larger extent when compared with the previous coating experiments and in the surface micrograph the layer looked almost completely dense. Probably, membrane coating on a substrate with a lower roughness could give SEM pictures with a completely dense layer, using this coating procedure.

As shown in Figures 9b (a) – (e), the same conclusions can be drawn for the sintering experiment at 1300°C. In the next sintering experiment at 1400°C, larger sintering grains were formed and a completely dense layer was obtained, which looked also completely tight in overview SEM pictures (Figure 9c (e)). The final thickness of the finished sintered layer measures ~ 1 – 1.5 μm .

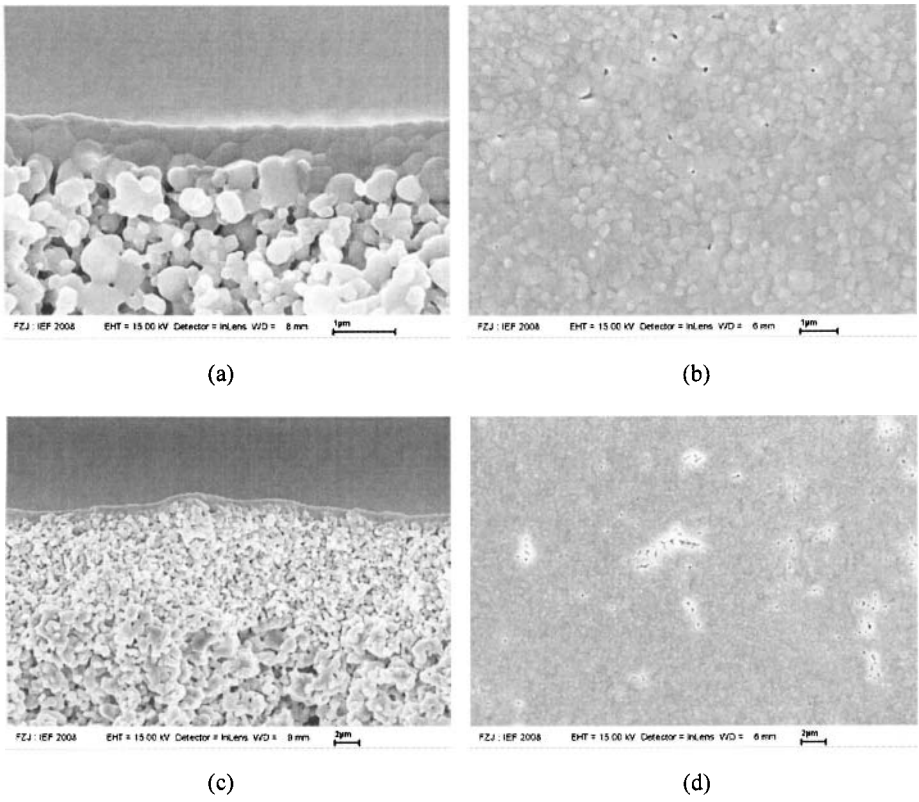

Fig. 9a (a) – (d). Micrographs of the cross-section and surface of the membrane shown in Fig. 8 after firing at 1200°C.
(Nano-dispersion, Colloidal sol: 2 x dip-coating and calcination at 500°C; (a,b) bar = 1 μm, (c,d) bar = 2 μm)

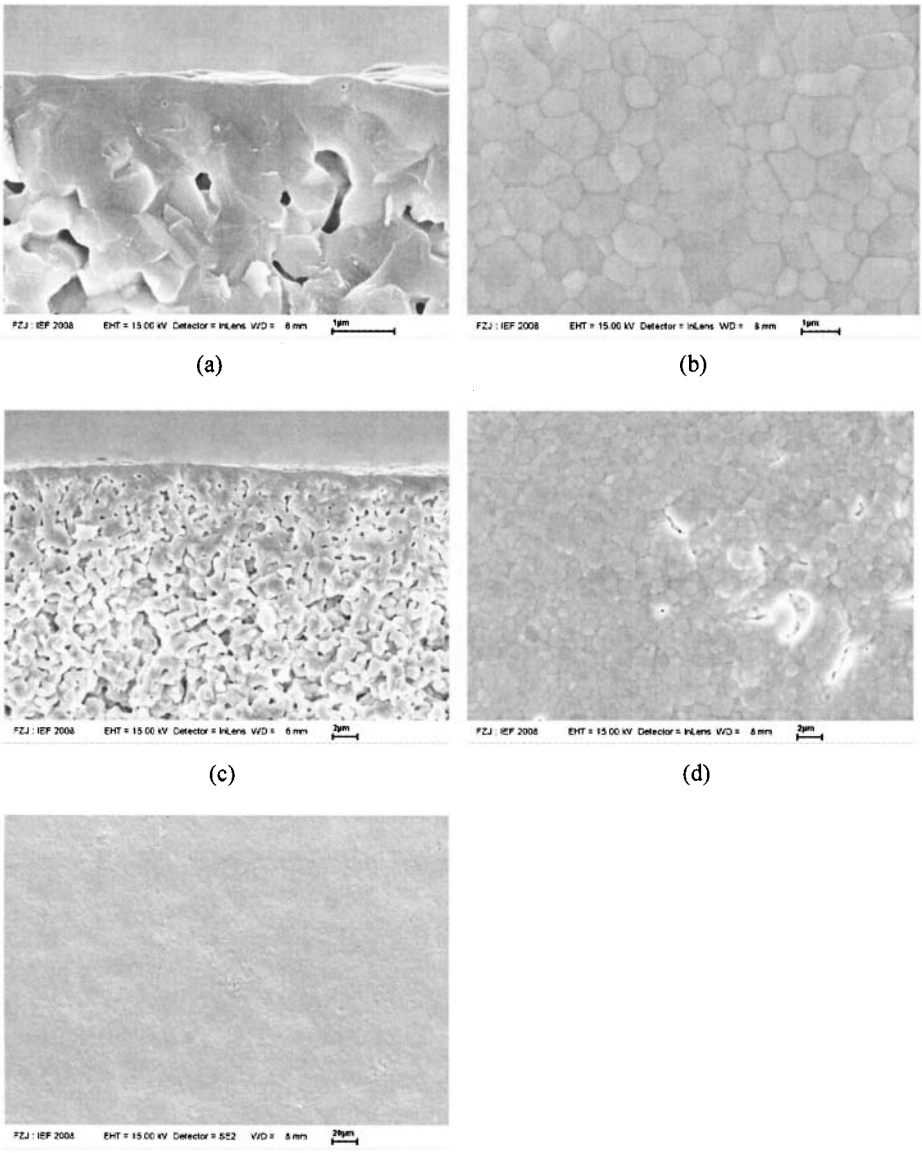

Fig. 9b (a) – (e). Micrographs of the cross-section and surface of the membrane shown in Fig. 8 after firing at 1300°C.
(Nano-dispersion, Colloidal sol: 2 x dip-coating and calcination at 500°C; (a,b) bar = 1 μm, (c,d) bar = 2 μm, (e) bar = 20 μm)